THE EFFECT OF AN EXTENSIONAL STRESS ON THE FLUCTUATIONS OF UNSTABLE FLOWS

Marcelo Andreotti
andreotti@unb.br

Rodrigo Avelino Mesquita dos Santos
rodrigo.avelino@bol.com.br

Aldo João de Sousa
aldo@unb.br

Francisco Ricardo da Cunha
frcunha@unb.br

Universidade de Brasília, Departamento de Engenharia Mecânica - FT
Campus Universitário Darcy Ribeiro, 70910-900 - Brasília, DF, Brazil

Abstract. *In this work, the effect of reducing unstable fluctuations in non-linear flows by the addition of anisotropic particles in a Newtonian incompressible fluid is examined. The particles produce an extensional stress in the flow that inhibits the efficiency of momentum transport by velocity fluctuations. This mechanism have produced a substantial drag reduction in pipe turbulent flows and attenuated gas bubble oscillations in a complex fluid. A theoretical model is developed based on a non-linear model that takes into account the extra rate of strain generated in the flow by the local orientation of the additives. An increase of the buffer layer thickness is observed by the measurements using laser doppler velocimeter (LDV). A numerical study is also developed for a bubble under a time dependent pressure field. Collapse and bifurcation diagrams show that the addition of a low concentration of particles in a viscous fluid undergoing an acoustic pressure may change significantly the non-linear motion of a bubble.*

Keywords*: anisotropic particles, fluctuations, drag reduction, bubble dynamics.*

1. Introduction

The physical mechanisms responsible for the phenomenon of instabilities attenuation by the presence of additive in the flow are not completely understood and remain a subject of debate. The role of stress anisotropy due to polymer extension versus elasticity in this mechanism is still ongoing subject of controversy. Several theories have been presented to explain these mechanisms. de Gennes, 1990 and Joseph, 1990 among other authors, suggest that elasticity is the main factor behind the stabilization of the flow fluctuations. Some authors support the theory that the main mechanism is associated with anisotropy arising from the local orientation of the polymer chains once they are fully stretched (e.g. Landhal, 1972; Hinch and Leal, 1976; den Toonder et al., 1997; Andreotti et al., 2002).

The application of direct numerical simulations (DNS) of turbulent flows has been used to demonstrate the drag reduction phenomenon. DNS of a fully turbulent channel flow of a dilute polymer solution developed by Dimitropoulos et al., 1998 have shown that the polymer induces several changes in the flow characteristics. In particular, these authors have observed a partial inhibition of turbulence generating events within the buffer layer by the macromolecule often onset of drag reduction.

Bubble dynamics in variable pressure fields has been widely studied since the classic work of Rayleigh, 1917. The motion of a spherical bubble developing radial motion under severe conditions presents a strong non-linear behavior and the bubble can even collapse. A collapsing bubble can reach high pressure and temperature that may produce serious consequences in various subjects, such as erosion in turbines and pumps, emulsification, molecular degradation and sonoluminescence. This phenomenon is subject of investigation in many works, such as Hammit, 1980, Knapp et al., 1970, Barber et al., 1997, Kameth and Prosperetti, 1989, Hao and Prosperetti, 1999. The use of additive in flows generated by cavitating bubbles has been discussed in the experimental works of Chahine, 1977, Chahine and Fruman, 1979. Ellis et al., 1970 have found out a reduction of 30% of incipient cavitation using solution of polymer additive such as Polyox WSR 301.

The aim of this work is to investigate the mechanism that attenuate fluctuations in turbulent flows and in the motion of an oscillatory bubble undergoing a chaotic motion promoted by the addition of a low concentration

of anisotropic particles. The theoretical model proposed in this article points out that a stress anisotropy created in both flows by the presence of additives reduces drastically the instabilities.

1.1. Scaling arguments

In this section we propose some scaling sarguments based on a dumb-bell model in order to predict the order of magnitude for the particle relaxation time. The model consists of two rigid spheres linked by a elastic spring. The restoring force due to the Brownian motion is represented by the spring and the viscous drag by the spheres. In the equilibrium condition, the drag force scales with the elastic Brownian force. So, a typical time scale is of the same order of the relaxation time of the polymer. Therefore, one obtains the relaxation time for the polymer macromolecule as (see Andreotti et al., 2002):

$$\tau \sim \frac{\mu\delta^3}{kT}\left(\frac{M_i}{M}\right)^{3/2}, \tag{1}$$

where δ is the length of a monomer, k the Boltzmann constant, T the fluid temperature, M is the molecular weight of the polymer and M_i the molecular weight of a monomer. Defining Db, the Deborah number, as the ratio between the relaxation time of the material, τ and the characteristic time scale of the flow t^*. It is reasonable to consider that the diameter of the polymer is the same order of magnitude that the length of a monomer. Hence, we can estimate an aspect ratio for a stretched polymer macromolecule, as follows

$$\frac{\ell}{\delta} \sim \frac{U\mu\delta^2}{kT}\left(\frac{M_i}{M}.\right)^{3/2}. \tag{2}$$

For the present work $\delta = 0.5nm$, $\mu = 1cp$, $M = 10^6 g/mol$, $M_i = 71 g/mol$, $k = 1.38 \times 10^{-23} J/K$, $T = 293K$ and $U = 3m/s$. In these typical conditions $\tau = O(10^{-5})s$ and $\ell/\delta = O(10^5)$.

2. Balance equations

The balance equations are the continuity equation and the Cauchy's equation. Generally they can be written as:

$$\nabla \cdot \mathbf{u} = \mathbf{0} \tag{3}$$

is the mass balance equation, where $\mathbf{u}$ is the Eulerian velocity field of the flow, and

$$\rho\left(\frac{\partial \mathbf{u}}{\partial t} + \mathbf{u}\cdot\nabla\mathbf{u}\right) = \nabla\cdot\boldsymbol{\Sigma} + \rho\mathbf{g} \tag{4}$$

is the momentum balance equation, where $\boldsymbol{\Sigma}$ is the fluid stress tensor and $\mathbf{g}$ is the gravity acceleration vector.

3. Constitutive equations

The constitutive model used in this work considers an incompressible fluid of viscosity μ and density ρ that contains a concentration ϕ of additives like long fibers or macromolecules of high molecular weight with aspect ratio ℓ/a. The particles are oriented by a unitary vector $\mathbf{s}$.

The stress tensor of the fluid $\boldsymbol{\Sigma}$ is described by a non-Newtonian model because the presence of additives causes a stress anisotropy in the flow what produces a non-linear effect. For a suspension of anisotropic particles is proposed the following equation:

$$\boldsymbol{\Sigma} = -p\mathbf{I} + \mathbf{2}\tilde{\mu}\mathbf{D} + \mathbf{2}\boldsymbol{\Sigma}_\mathbf{f}, \tag{5}$$

where p is the fluid pressure, $\mathbf{I}$ is the isotropic unitary tensor, $\tilde{\mu}$ is the shear viscosity of the suspension composed by the polymer additive and the ambient fluid, $\mathbf{D} = \frac{\mathbf{1}}{\mathbf{2}}\left(\nabla\mathbf{u} + (\nabla\mathbf{u})^\mathbf{T}\right)$ is the rate of strain tensor and Σ_f, the extra stress tensor due to the additives. The shear viscosity of the suspension $\tilde{\mu} = \tilde{\mu}(\dot{\gamma}, \phi)$, *i.e.* $\tilde{\mu}$ is a function of the shear rate $\dot{\gamma}$ and the volume fraction of the additive ϕ. For dilute suspension, $\tilde{\mu} \approx \tilde{\mu}(\phi)$ and can be simply calculated by the expression $\tilde{\mu}(\phi) = \mu(1 + A\phi)$, proposed by Einstein, 1956. In this work, the value of the constant A is determined experimentally. A second order correction has been also considered based on Batchelor and Green Theory (1972).

The model for $\boldsymbol{\Sigma}_\boldsymbol{f}$ is based on a particular case of the general formulation proposed by Hinch and Leal, 1976 for a suspension of anisotropic particles free of inertia, sedimentation and Brownian motion. In addition

the axial deformation of the particles is supposed much smaller than its thickness. Under the above condition one obtains:

$$\mathbf{\Sigma}_f = \mu_e(\mathbf{s}\cdot\mathbf{D}\cdot\mathbf{s})\mathbf{ss}. \tag{6}$$

$\mathbf{\Sigma}_f$ is physically interpreted as an extra stress in the additive orientation direction, say $\mathbf{s}$, that is proportional to the rate of strain tensor component $\mathbf{s}\cdot\mathbf{D}\cdot\mathbf{s}$ in such direction. This term represents the macroscopic average contribution of the additive to the fluid stress with μ_e being an extensional viscosity due to the extensibility of the particle. Polymer macromolecule or long fiber tends to resist to stretching along its own axis. The extensional viscosity μ_e characterizes the importance of this resistance. Figure 1 illustrates the proposed extensional viscosity model.

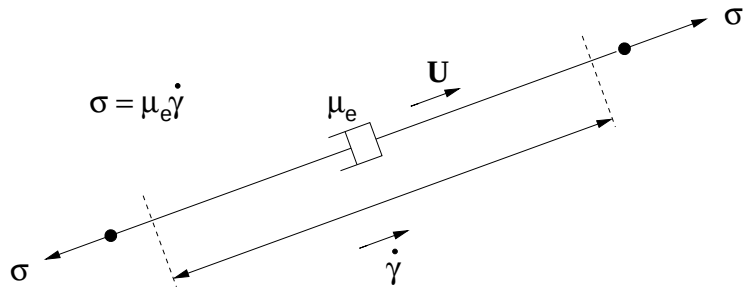

Figure 1: An extensional viscosity produced by the extensibility of additives by the flow.

In this study it is considered long aspect ratio fibers (ℓ/a) or high molecular weight polymers. These additives present a high relaxation time. Here ℓ and a are the length and diameter of the particle, respectively. The relaxation time of the polymer macromolecules is much larger than the characteristic time τ of the flow. As showed in section 1.1, $\tau \sim O(M^{3/2})$ and $M \sim O(10^6 g/mol)$. The monomers of those molecules remain extended and supposing they do not degrade, they behave, approximately, in a similar way of fibers of large aspect ratio.

4. Suspension rheology

In the present section, the material function $\mu_e/\tilde{\mu}$ is defined for different regimes of particle volume fraction. The assumption of particles aligned locally with the main flow direction is used. This consideration is acceptable when the time to change the additive orientation is much smaller than convective time scale of the flow. Under these circumstances $\mathbf{s} = \mathbf{u}/|\mathbf{u}|$. Batchelor, 1970 based on a slender body theory has predicted that for dilute suspension of rigid rods or long fibers

$$\mu_e/\tilde{\mu} = \frac{4\pi}{3}\frac{(n\ell^3)}{\ell n(\ell/a)} \qquad (n\ell^3 \ll 1), \tag{7}$$

where n is the density number of particles in the suspension. It might be important to notice that the analogy of polymer chains with a suspension of long rigid fibers or rods seems to be a reasonable model for polymers of high molecular weight (long relaxation time). Equation (7) shows that for a suspension of long fibers or stretched molecules there is an important effect proportional to $n\ell^3$. Shaqfeh and Frederickson, 1990 proposed a rigorous asymptotic theory to describe the function $\mu_e/\tilde{\mu}$ for semi-dilute regimes, *i.e.* $\phi \ll 1 \ll n\ell^3$. This theory takes into account a first order effect of two-particles hydrodynamic interaction. For cylindrical fibers, considered here, $n\ell^3 = (\phi/\pi)(\ell/a)^2$, the dimensionless expressions for extensional viscosity models are expressed as follows:

$$\frac{\mu_e}{\tilde{\mu}} = \begin{cases} \frac{4}{3}\left(\frac{\ell}{a}\right)^2 \frac{\phi}{\ln(\ell/a)}, & \text{if } n\ell^3 \ll 1 \\ \frac{4}{3}\left(\frac{\ell}{a}\right)^2 \frac{\phi}{\ln(1/\phi)}\left(1 - \frac{\ln(\ln(1/\phi))}{\ln(1/\phi)} + \frac{E(\phi)}{\ln(1/\phi)}\right), & \text{if } \phi \ll 1 < n\ell^3 \end{cases} \tag{8}$$

where $E(\phi) = 0.1585$ for cylindric shape particles aligned to the flow.

4.1. Polymeric solution rheometry

The result of the rheological characterization of the Polyacrilamide solution used in the experiments and theory is described here. The influence of the shear rate on the shear viscosity of the polymeric solution is presented in Fig. 2.

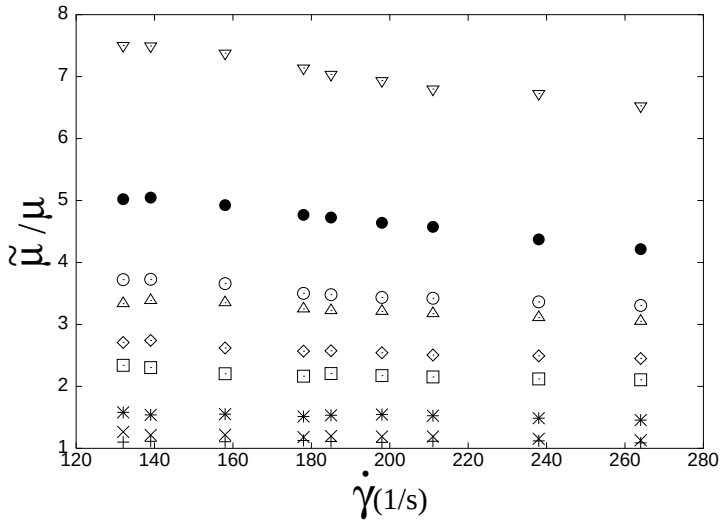

Figure 2: Dimensionless shear viscosity of the Polyacrilamide solution as a function of shear rate. The points represents: $+$ $\phi = 0$, $\times$ $\phi = 20ppm$, $\star$ $\phi = 40ppm$, $\square$ $\phi = 80ppm$, $\diamond$ $\phi = 120ppm$, $\triangle$ $\phi = 200ppm$, $\circ$ $\phi = 300ppm$, $\bullet$ $\phi = 350ppm$ e $\bigtriangledown$ $\phi = 450ppm$.

It is seem that the shear viscosity of the polymer solution is approximately constant for shear rates, $\dot{\gamma}$, beyond 180 s^{-1} at all concentrations. This behavior is similar to Boger fluids which have a constant shear viscosity over a wide range of shear rates. The constant value of shear viscosity is observed to be about three times lager than the viscosity of the solvent at 200 ppm of the Polyacrilamide. For a polymer concentration of 450 ppm the shear viscosity is observed to be approximately eight times larger than the viscosity of the solvent in the limit of $\dot{\gamma} \mapsto 0$. Of course it contributes to an increase in the friction factor of the flow in contrast with the drag reduction promoting by enhanced of the extensional viscosity of the polymer solution. As seem in Fig. 2, for the larger concentration used a shear thinning behavior is clearly identified, i.e. the shear viscosity of the polymeric solution decrease as a function of shear rate.

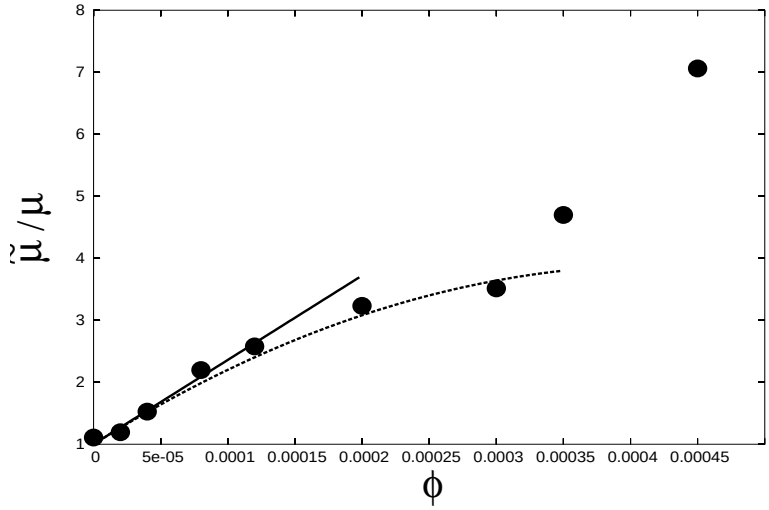

Figure 3: Dimensionless shear viscosity of the Polyacrilamide solution as a function of the additives concentration. The full-line fits the experimental data with the Einstein theory (1956) and the dashed-line refers to the theory developed by Batchelor and Green, 1972.

Figure 3 shows that for a volumetric concentration up to 0.00013 (130 ppm) of Polyacrylamide the hydrodynamic interactions between the macromolecules can be neglected, resulting in a linear behavior of the shear viscosity with the particle concentration. In these regimes, the contribution associated with the shear viscosity of the polymer solution is treated as a Newtonian equivalent fluid of viscosity $\tilde{\mu}$, with a energy dissipation

larger then the solvent. At low concentrations each macromolecule behaves as a single particle, with no hydrodynamic disturbance that influences the motion of the neighborhood. This effect can be predicted by Einstein's linear expression, defined before, $\tilde{\mu} = \mu(1 + A\phi)$, with $A = 13600$. However, when the additive concentration increases, the linear regime is no longer observed. For the volumetric concentration of Polyacrylamide varying from 130 to 300 ppm, the effective shear viscosity may be described by second order theory given by Batchelor and Green, 1972, namely $\tilde{\mu} = \mu(1 + A\phi + B\phi^2)$, for $B = -1.6 \times 10^8$. The values of the constants A and B were determined from our experimental data. The non-linear behavior $O(\phi^2)$ of the shear viscosity can be explained by the hydrodynamic interactions among the additive orientation that cause a significant change in the rheology of the polymeric solution. This theory breaks in the limit ($\phi \simeq 350ppm$) when it is also observed an increase in the friction factor in contrast with the decreasing promoted by the extensibility of the additives.

5. Drag reduction

In this section we present some experimental results of drag reduction in turbulent pipe flow. The experiments were conducted in the Department of Mechanical Engineering at University of Brasília (see Andreotti et al., 2002). The additive used in the experiments was an aqueous polymer solution with a volumetric concentration of 30% of an ionic high molecular weight Polyacrylamide ($10^6 g/mol$).

In our previous work Andreotti et al., 2002 a theoretical expression for the friction factor of the turbulent pipe flow has been derived, namely:

$$f = \left[\frac{7\sqrt{2}}{16} + \frac{5\sqrt{2}}{8} \left(\ln(r_0^+) + \frac{C}{Re} \left(\frac{\ell}{b} \right)^2 \frac{\phi}{\ln(1/\phi)} \left(1 - \frac{\ln(\ln(1/\phi))}{\ln(1/\phi)} + \frac{E(\phi)}{\ln(1/\phi)} \right) \right) \right]^{-2}. \tag{9}$$

The formula above depends on the concentration and aspect ratio of the additives. Here $r_0^+ = r_0 u_f/\nu$ being r_0 is the radius of the tube, u_f is the friction velocity of the flow, ν is the kinematics viscosity, C is a constant of calibration and Re is the Reynolds number.

Figure 4 shows a comparison between experimental data and the results calculated by the theoretical formula proposed in the eq. (9). The plot shows the friction factor as a function of concentration for a Re=10^5 and $\ell/a \sim 10^5$. Note that for $C = O(1)$ the model fits the experimental data with good accuracy for the full range of concentrations.

bugbug

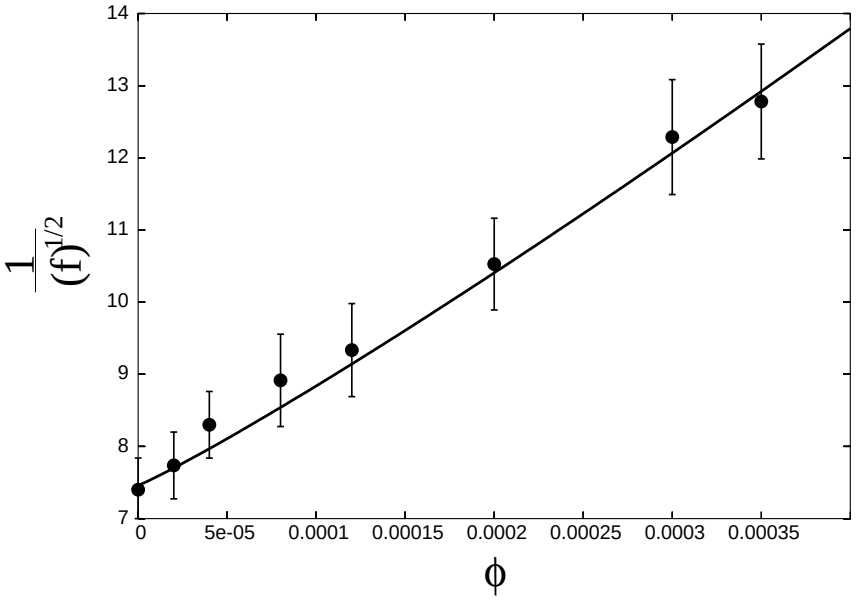

Figure 4: Comparison of the experimental data with the model proposed for Re=10^5 and $\ell/a \sim 10^5$.

Figure (5) presents dimensionless mean velocity profiles as a function of the wall distance for a Reynolds number 3.3×10^3 based on the friction velocity. The laser doppler velocimeter (LDV) measurements for pure water ($\phi = 0$) is fitted by the Kárman-Prandtl universal logarithmic law, whereas the mean velocity

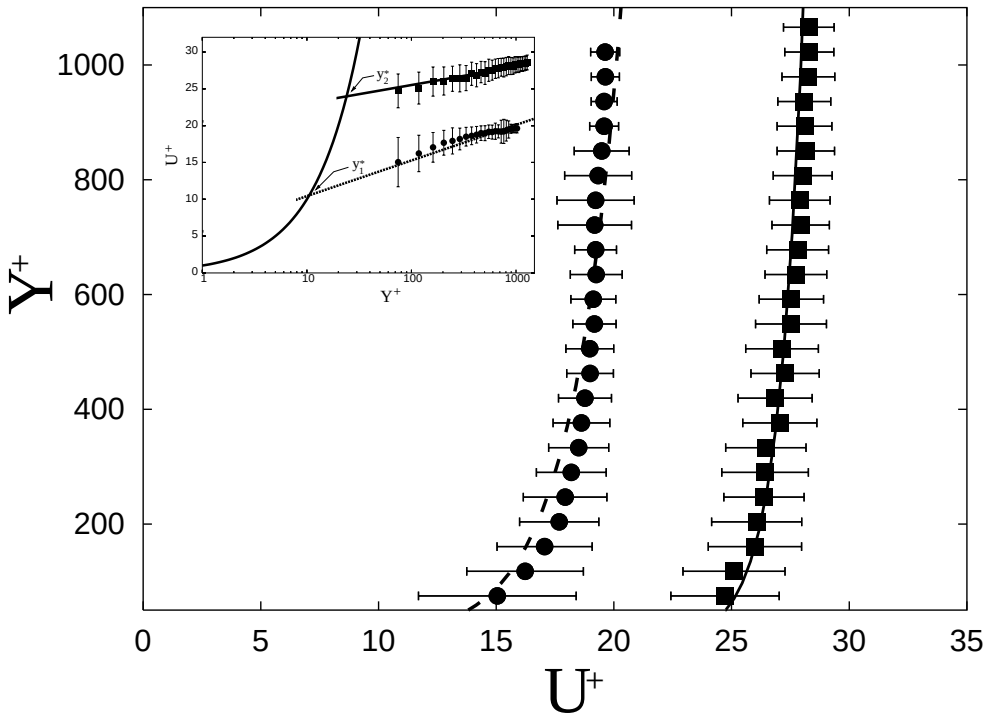

Figure 5: The experimental and theoretical mean flow velocity as a function of wall distance. The symbols • represents pure water $\phi = 0$ and the symbols ■ represents a polymeric solution ($\phi = 120ppm$). The dashed-point line is the Kárman-Prandtl universal logarithmic law and dashed line is the theoretical model for ($\phi = 120ppm$) and $\ell/a = 10^5$.

measurements for a polymer solution of 120 ppm of Polyacrylamide are fitted by our theoretical model for the mean velocity profile of the turbulent flow, namely:

$$u^+ = u^+_{max} + \frac{1}{\kappa(1+\epsilon)^{1/2}} \ln(y^+) - \frac{1}{\kappa(1+\epsilon)^{1/2}} \ln(r_0^+) \tag{10}$$

where $\kappa = 0.4$ is Kárman universal constant for smooth pipes, $\epsilon = \mu_e/\mu Re$ and r_0^+ is the dimensionless tube radius. For our experimental data the eq. (10) can be written as: $u^+ = 1.07\ln(y^+) + 20.56$.

It is seen that the addition of the polymer reduces the intensity of the wall eddies and increase their average size. Consequently there is an increase in the thickness of the buffer layer. The thickness of the buffer layer is defined here as the value y^* at which the extrapoled viscous and the inertial sublayer profiles intersect. The insert in Fig. 5 presents a detail of the increase in the thickness of the buffer layer in a monolog scale. For pure water, the thickness of the buffer layer corresponding to $y_1^* \approx 11$ and for a polymer solution $y_2^* \approx 24$ (i.e. $y_2^*/y_1^* \cong 2$). The reduction in the intensity of the wall eddies, provides evidence for a mechanism of drag reduction based on the inhibition of the wall eddies since they facilitates significant amounts of the turbulence production. These observations are also consistent with the mechanism of drag reduction requiring a significantly enhanced extensional viscosity in the flow resulting in the suppressing of the eddies which carry the Reynolds stress in the buffer layer.

6. Bubble dynamics

Next, the effect of addition of a small concentration of anisotropic particles in reducing the non-linear motions of a cavitating bubble is explored by numerical simulation of a modified *Rayleigh-Plesset equation* for the case of non-Newtonian fluid.

In the present study is considered a neutrally buoyant bubble filled with an ideal gas of initial radius R_0 developing a radial oscillatory motion in a suspension of anisotropic particles. The equation that governs this kind of motion is the well-known *Rayleigh-Plesset equation* (see Plesset and Prosperetti, 1977,). We use the

extension of this equation developed in our previous work, Santos et al., 2002, namely:

$$R\ddot{R} + \frac{3}{2}\dot{R}^2 = \frac{2}{We}\left[\frac{1}{R^{3n}} - \frac{1}{R}\right] - \frac{4}{Re}\left[1 + \langle f(\phi, \ell/a, r, \theta)\rangle\right]\frac{\dot{R}}{R} - \left[1 + \varepsilon sin(\omega t)\right] + \frac{1}{R^{3n}} \tag{11}$$

where We is the Weber number defined as the ratio between inertial forces and surface tension forces, *i.e.* $We = \rho R_E U_c^2/\sigma$; Re, the Reynolds number, refers to the competition between inertial and viscous effects, i.e. $Re = \rho R_E U_c/\mu$, n is the polytropic coefficient, ω the frequency of the forcing pressure and ε its dimensionless amplitude. U_c is a characteristic velocity scale defined as $((\tilde{P}_\infty - P_v)/\rho)^{\frac{1}{2}}$ and R_E is the equilibrium radius of the system. $\tilde{P}_\infty$ is the equilibrium far field pressure and P_v is the pressure of the vapor inside the bubble. More details of this model are given in our recent work (Santos et al., 2002).

Figure 6 shows a typical nonlinear response of the bubble motion for two different configurations in the absence of additives. In Fig. 6.a, the bubble oscillates under condition of $Re = We = 7$, pressure amplitude $\varepsilon = 1.5$ and $\omega = 1.0$. The dashed line is the harmonic pressure forcing and the full line corresponds to the bubble radius time evolution . It is seen that the bubble response is not harmonic in a period of oscillation. Figure 6.b is a phase diagram of the motion ($\dot{R} \times R$). The figure in this plot indicates the stability configuration of the system. The complex picture of the trajectory attractor in this kind of plot indicates the existence of extra degree of freedoms characterized by different periods of oscillation.

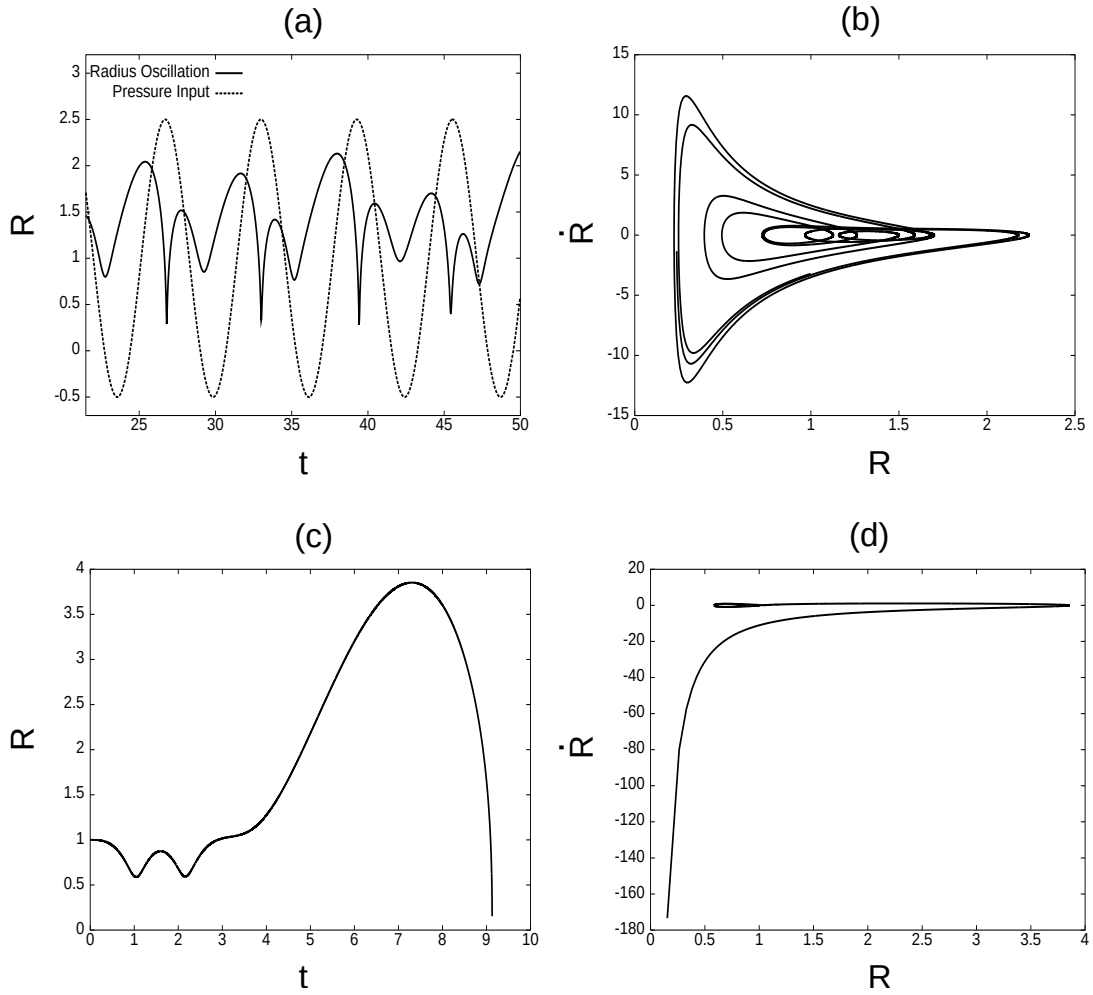

Figure 6: Nonlinear response of a bubble motion under two different configurations. The plots (a) and (b) are for $Re = 7$, $We = 7$, $\varepsilon = 1.5$ and $\phi = 0$. (a) is the radius of the bubble (filled line) and the pressure forcing (dashed line) as a function of time; (b) shows the phase diagram. The plots (c) and (d) are for $Re = 1200$, $We = 200$, $\varepsilon = 3.0$ and $\phi = 0$, (c) is the radius of the bubble and (d) shows the phase diagram.

A limit circle in this kind of plot would indicate simply a linear or harmonic motions of the system. Thus such configuration is unstable. A more severe condition is presented in Fig. 6.c and Fig. 6.d. The set of

parameters, $Re = 1200$, $We = 200$, pressure amplitude $\varepsilon = 3.0$ and $\omega = 1.0$, leads the bubble to collapse. Under these conditions the bubble oscillations persist only for a short time. It grows for a value of the radius around 3.5 and then contract rapidly reaching the minimum value of R corresponding to the van der Walls hard core. This value is the limit of maximum packing of the molecules of the gas inside the bubble. According to Knapp et al., 1970, a reasonable dimensionless minimum radius is $0.1R$. The phase diagram in the collapse is opened as shown in Fig. 6.d.

Now, we consider the addition of a low concentration ϕ of anisotropic particles in the fluid outside the bubble. Shaqfeh and Frederickson, 1990 model has been used for the extensional viscosity. Figure 7 shows the bubble history and the phase diagram for the collapse conditions and $\phi = 20$ ppm. It is seen that the bubble does not collapse and the bubble oscillatory motion behavior is much less unstable. A slightly instability can be seen in the phase diagram. The motion tends to a limit cycle in this diagram and the amplitude of the bubble motion takes the same value after $t \sim 50$. Another characteristic to be noticed is the dramatic decreasing of the amplitude of the bubble oscillations in presence of additives. For further increase in the concentration the motion becomes more and more stable and the amplitudes much smaller. Figure 8 shows these findings. Figure 8.a presents the phase diagram for the collapse condition and Fig. 8.b shows the phase diagram for six different concentrations varying in the range of $20 - 350$ ppm of polymer in the solution.

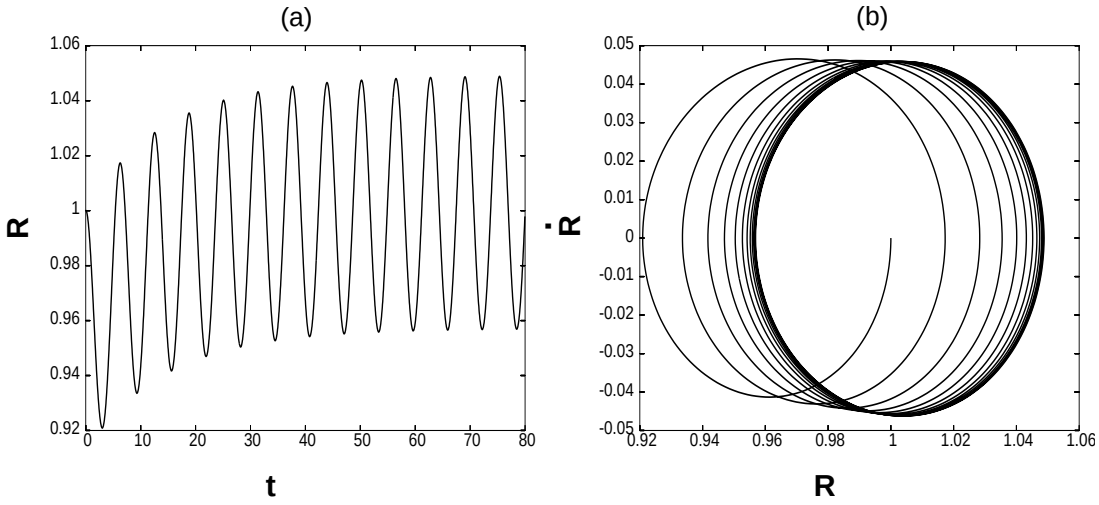

Figure 7: History of the bubble motion for $Re = 1200$, $We = 200$, $\phi = 20$ ppm and $\ell/a \sim 10^5$. (a) $R \times t$ and (b) $\dot{R} \times R$.

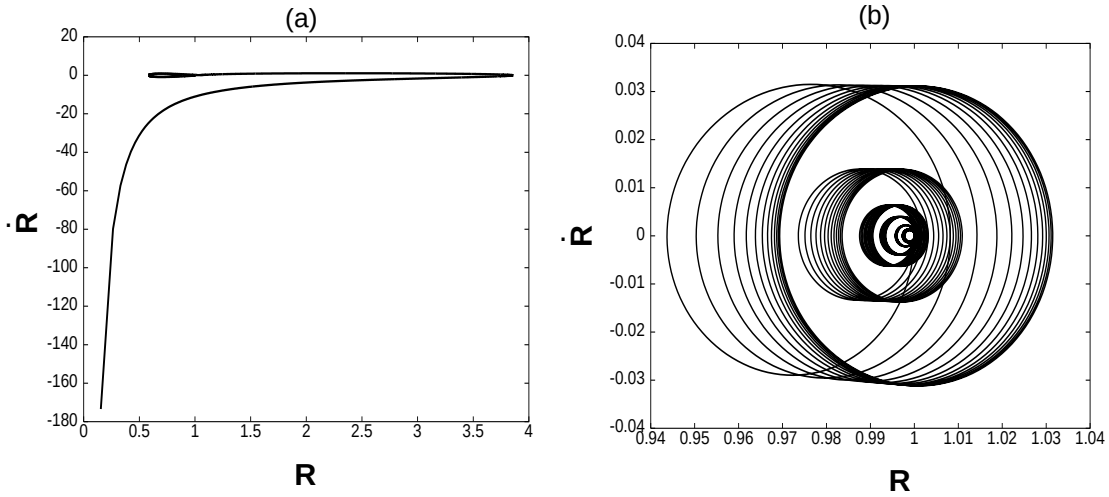

Figure 8: Phase diagrams for $Re = 1200$, $We = 200$ and $\varepsilon = 3.0$. (a) corresponds to the collapse condition and (b) shows the Polyacrilamide effect on the stabilization of the motion for the range of concentration 20 ppm $\leq \phi \leq$ 350 ppm

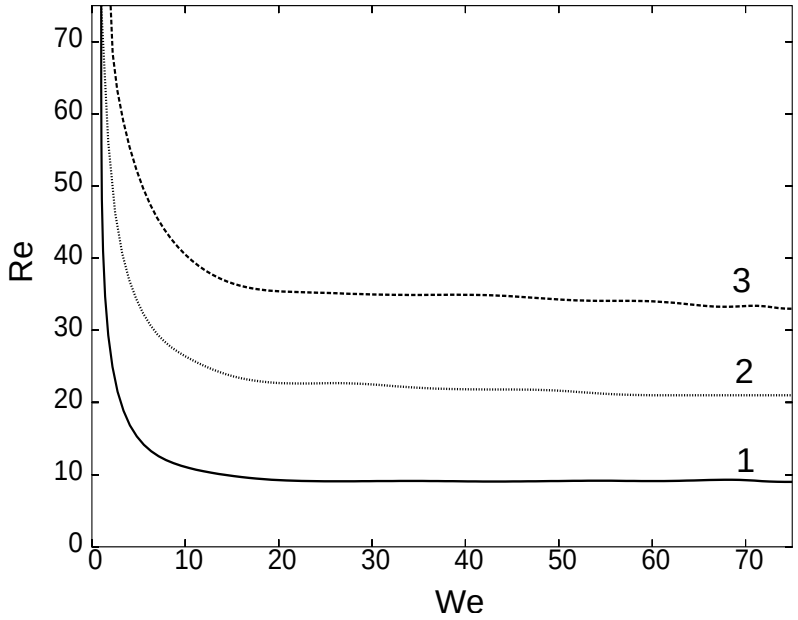

Figure 9: Collapse diagram $\varepsilon = 1.5$. Influence of the models for the extensional viscosity. $1 \rightarrow$ collapse line in the absence of fibers; $2 \rightarrow$ collapse line using Shaqfeh and Frederickson, 1990 model; $3 \rightarrow$ collapse line using Batchelor, 1970 model.

A plot of $Re \times We$ is interesting to show the collapsing behavior of the system in terms of a range of Re and We. We have interpreted this result as a collapse diagram. The diagram shows the collapse and non-collapse regions separated by a line that represents the collapse threshold for a given set of parameters. Figure 9 presents a comparison between the collapse lines for the two different models of extensional viscosity $\mu_e/\tilde{\mu}$ given in eq. 8 . All results are for $\ell/a = 100$, $\phi = 1000$ ppm and $\omega = 1.0$. Line 1 shows the collapse limit for the bubble in the absence of additives. It is seen that the collapse domain covers a much larger region than the non-collapse domain. Line 2 corresponds to the collapse threshold in the presence of additives considering Shaqfeh and Frederickson, 1990 model. The non-collapse region is increased by approximately 2 times. This model takes into account the first order effect of interactions between the additives. Batchelor's model (1970), corresponds to line 3. The later model does not take into account any hydrodynamic interactions between particles and the non-collapse region is about 60% larger then the size of the non-collapsing domain predict by the extensional viscosity using Shaqfeh and Frederickson model. It seems that a slightly additive re-orientation produced by the hydrodynamic interaction attenuates the effect of the molecule stretching on the flow. Consequently, the hydrodynamic interactions between pair of fibers avoid each particle orienting in the flow direction and, thus the bulk stabilization effect is decreased.

7. Final remarks

The effect of anisotropic particles on unstable flows has been investigated in this work. It could be seen that the presence of fibers or macromolecules of high molecular weight reduces drastically the fluctuating behavior in a turbulent pipe flow and in a motion of an oscillating bubble.

Bubble dynamic simulations have shown that even for critical situation like collapse the motion is stabilize by the addition of a low concentration of polymer macromolecules. The phase diagrams presented have confirmed this effect of stabilization. We have also tested extensional viscosity models in terms of a collapse diagram. It was showed that the model proposed by Shaqfeh and Frederickson, who considers a first order correction of the hydrodynamic inter-particles interaction the non-collapse region around 1.3 times less than Batchelor, 1970 model.

Significant evidence has been provided on the role of an enhanced extensional viscosity of a polymer solution in promoting a effect of stabilization. The effect of reducing fluctuations in both flows tested here can be a direct consequence of an anisotropic answer of the flow to an anisotropic viscosity induced by the macromolecule stretching.

8. References

Andreotti, M., Cunha, F. R., and Sousa, A. J., 2002, A Theoretical and Experimental Study of the Drag Reduction Phenomenon in Turbulent Flows, "Prodedings of the 9^{th} Brazilian Congress of Thermal Engineering and Sciences", Vol. Paper CIT02-0749, pp. 1–12, Caxambu, MG, Brazil.

Barber, B. P., Hiller, R. A., Lofsdedt, R., Putterman, R., and Weninger, K. R., 1997, Defining the Unknown of Sonoluminescence, "Phys. Reports", Vol. 281, pp. 80–82.

Batchelor, G. K., 1970, Slender-body Theory for Particle of Arbitrary Cross Section in Stokes Flow, "Journal of Fluid Mechanics", Vol. 44, pp. 813.

Batchelor, G. K. and Green, J. T., 1972, The determination of the Bulk Stress in a Suspension of Spherical Particles to Order C^2, "Journal of Fluid Mechanics", Vol. 56, pp. 401–427.

Chahine, G. L., 1977, Interaction Between an Oscillating Buble and a Free Surface, "Journal of Fluids Engineering", Vol. 99, pp. 709–716.

Chahine, G. L. and Fruman, D. H., 1979, Dilute Polymer Solution Effects on Buble Growth and Collapse, "Physics of Fluids", Vol. 22(7), pp. 1406–1407.

de Gennes, P. G., 1990, "Introduction to Polymer Dynamics", Cambridge University Press, England.

den Toonder, J. M. J., Hulsen, M., Kuiken, G., and Nieuwstadt, F., 1997, Drag Reduction by Polymer Additives in a Turbulent Pipe Flow: Numerical and Laboratory Experiments, "J. Fluid Mech.", Vol. 337, pp. 193–231.

Dimitropoulos, C. D., Sureshkumar, R., and Beris, A. N., 1998, Direct Numerical Simulation of Viscoelastic Turbulent Channel Flow Exhibiting Drag Reduction: Effect of the Variation of Rheological Parameters, "J. Non-Newtonian Fluid Mech.", Vol. 79, pp. 433–468.

Einstein, A., 1956, "Investigations to Polymer Dynamics", Dover, New York.

Ellis, A. T., Waugh, J. F., and Ting, R. Y., 1970, "Journal of Basic Engineering", Vol. 92, pp. 459.

Hammit, F. G., 1980, "Cavitation and Multiphase Flow Phenomena", Ed. McGraw-Hill, New York, United States.

Hao, Y. and Prosperetti, A., 1999, The Dynamics of Vapor Bubbles in Acoustic Pressure Fields, "Phys. Fluids", Vol. 11, pp. 2008–2019.

Hinch, E. J. and Leal, L., 1976, Constitutive Equations in Suspension Mechanics, "Journal of Fluid Mechanics", Vol. 76, pp. 187–208.

Joseph, D. D., 1990, "Fluid Dynamics of Viscoelastic Liquids", Springer.

Kameth, V. and Prosperetti, A., 1989, A Numerical Integration Methods in Gas-Bubble Dynamics, "J. Acoust. Soc. Am.", Vol. 85, pp. 1538–1548.

Knapp, R., Daily, J., and Hammit, F., 1970, "Cavitation", Ed. McGraw-Hill.

Landhal, M. T., 1972, "Drag Reduction by Polymers Additive", Ed. E. Becher & G. R. Mikhai 100, Springli.

Plesset, M. S. and Prosperetti, A., 1977, Bubble Dynamics and Cavitation, "Ann. Review of Fluid Mech.", Vol. 9, pp. 145–185.

Rayleigh, L., 1917, On the Pressure Developed in a Liquid During the Collapse of a Spherical Cavity, "Phil. Magazine", Vol. 34, pp. 94–98.

Santos, R. A. M., Cunha, F. R., and Sousa, A. J., 2002, The Complex Motion of a Gas Bubble in a Nonlinear Fluid, "Prodedings of the 9^{th} Brazilian Congress of Thermal Engineering and Sciences", Vol. Paper CIT02-0831, pp. 1–12, Caxambu, MG, Brazil.

Shaqfeh, E. S. G. and Frederickson, G. H., 1990, The Hidrodynamic Stress in a Suspension of Rods, "Journal of Physical Fluids", Vol. 2, pp. 7–24.